GeoStudio Example File
Transport and Consumption of Oxygen in Cover Material

To see the latest GeoStudio learning content, visit Seequent Learning Centre and search the catalogue for “GeoStudio”.

Seequent, The Bentley Subsurface Company

Introduction

Acidic leachate is produced when oxidation of sulphide occurs in an unsaturated system through which water transport is occurring. Soil cover systems with capillary barrier effects are often built to limit oxygen ingress towards mine wastes containing sulphide. Layers within the soil cover system that have a high water retention capacity also have a low coefficient of diffusion, which limits oxygen ingress. Constructing the water retaining layer from tailings that consume oxygen has the added benefit of limiting oxygen transfer deeper into the mine wastes. The objective of this example is to analyze oxygen transport through an unsaturated cover system and explore the effectiveness of oxidation within the water retention unit.

Background

Gas transport in unsaturated soils can be described mathematically to varying degrees of rigor. CTRAN/W is formulated based on a rather generalized form of the gas transfer equation that considers hydrodynamic dispersion and advection of a gas species in the gas and dissolved phases:

$$\theta_{eq}\frac{\partial C}{\partial t} = \frac{\partial}{\partial y}\left[\left(D_a\theta_a + D_w H\theta_w\right)\frac{\partial C}{\partial y}\right] - q_a\frac{\partial C}{\partial y} - Hq_w\frac{\partial C}{\partial y} - K_r^*\theta_{eq}C - \lambda\theta_{eq}C \qquad \text{Equation 1}$$

where D_a and D_w are the coefficients of hydrodynamic dispersion for gas transport in the gas and dissolved phases, respectively, C is the concentration, θ_a is the volumetric air content, H is the dimensionless form of Henry's equilibrium constant (i.e. concentration of gas in solution divided by concentration of gas above solution), θ_w is the volumetric water content, q_a is the air flux, q_w is the water flux, K_r^* is the bulk reaction rate coefficient for irreversible first order reaction processes such as oxidation, and λ is the decay constant for radioactive decay or some reaction rate coefficient for biodegradation or hydrolysis. The equivalent diffusion porosity is defined as:

$$\theta_{eq} = \theta_a + H\theta_w \qquad \text{Equation 2}$$

The coefficients of hydrodynamic dispersion comprise both the coefficient of mechanical dispersion, $D' = \alpha v$, and the bulk diffusion coefficient, D_d^*, for each phase:

$$D_w = \alpha v_w + D_{dw}^* \qquad \text{Equation 3}$$

and

$$D_a = \alpha v_a + D_{da}^* \qquad \text{Equation 4}$$

where $v_w = q_w/\theta_w$ is the gas front velocity in the dissolved phase, and $v_a = q_a/\theta_a$ is the gas front velocity in the gas phase. In diffusion dominated systems in which the gaseous species does not decay, the transport equation simplifies to:

$$\theta_{eq}\frac{\partial C}{\partial t} = \frac{\partial}{\partial y}\left[\left(D_{da}^*\theta_a + D_{dw}^* H\theta_w\right)\frac{\partial C}{\partial y}\right] - K_r^*\theta_{eq}C \qquad \text{Equation 5}$$

The use of a single bulk diffusion coefficient, D_d^*, is often convenient for the purposes of developing analytical solutions for well-defined and relatively simple conditions (Mbonimpa et al. 2003):

$$\theta_{eq}\frac{\partial C}{\partial t} = \frac{\partial}{\partial y}\left[D_d^*\theta_{eq}\frac{\partial C}{\partial y}\right] - K_r^*\theta_{eq}C \qquad \text{Equation 6}$$

or then again

$$\theta_{eq}\frac{\partial C}{\partial t} = \frac{\partial}{\partial y}\left[D_e\frac{\partial C}{\partial y}\right] - K_eC \qquad \text{Equation 7}$$

where $D_e = D_d^*\theta_{eq}$ is the effective diffusion coefficient and $K_e = K_r^*\theta_{eq}$ is the effective reaction rate coefficient. Obtaining the required inputs for the case where D_d^* is known can be done in one of three ways:

1. Assume all diffusion transport is through the gas phase (i.e. $D_{dw}^* = 0.0$) and calculate D_{da}^* from $D_{da}^*\theta_a = D_e$;
2. Assume all diffusion transport is through the dissolved phase (i.e. $D_{da}^* = 0.0$) and calculate D_{dw}^* from $D_{dw}^*H\theta_w = D_e$; or
3. Assume diffusion transport through both phases and estimate the bulk diffusion coefficient through one phase from a closed-form estimation technique. The bulk diffusion coefficient through the other phase is then calculated from the equality $D_e = D_{da}^*\theta_a + D_{dw}^*H\theta_w$.

There are several closed-form equations to estimate the diffusion coefficient. For example, Aachib et al. (2004) provided the following estimation for oxygen:

$$D_e = \frac{1}{n^2}\left(D_a^o\theta_a{}^x + D_w^oH\theta_w{}^y\right) \qquad \text{Equation 8}$$

where n is the porosity, $D_a^o \cong 1.8\times10^{-5}$ m²/s is the free phase diffusion coefficient for oxygen in air, $D_w^o \cong 2.5\times10^{-9}$ m²/s is the free phase diffusion coefficient for oxygen in water, $x = A\theta_a^3 - B\theta_a^2 + C\theta_a + D$, $y = A\theta_w^3 - B\theta_w^2 + C\theta_w + D$, and A, B, C, D are empirical constants equal to 1.201, 1.515, 0.987, and 3.119, respectively. In this case, D_{da}^* can be calculated from $D_{da}^*\theta_a = \left(D_a^o\theta_a{}^x\right)/n^2$ while D_{dw}^* can be calculated from $D_{dw}^*H\theta_w = \left(D_w^oH\theta_w{}^x\right)/n^2$.

Numerical Simulation

Mbonimpa et al. (2003) simulated oxygen diffusion and consumption through a cover system with capillary barrier effects. The cover system comprised different configurations of silt tailings between two sand layers. The silt tailings layer was assumed to retain water under the prevailing conditions and therefore provide the resistance to oxygen ingress. Table 1 provides a summary of the geometry and material properties, such as layer thickness, porosity, void ratio, dry density, degree of saturation, equivalent diffusion porosity, effective and bulk diffusion coefficients and the effective reaction rate coefficient. The volumetric water content (or degree of saturation) of each layer was assumed constant, allowing for the use of constant transport and consumption coefficients.

Table 1. Properties of the three-layer covers (Mbonimpa et al., 2003).

Material	L [m]	n	S [%]	θ_{eq}	D_e [m²/s]	D_d* [m²/s]	K_e [1/s]
Case A							
Sand	0.30	0.29	13.50	0.2520	2.28×10^{-6}	9.05×10^{-6}	0
Tailings	0.60	0.46	83.10	0.0890	2.42×10^{-8}	2.72×10^{-7}	0
Sand	0.40	0.29	28.30	0.2104	1.27×10^{-6}	6.04×10^{-6}	0
Case B							
Sand	0.25	0.33	8.90	0.3015	3.10×10^{-6}	1.03×10^{-5}	0
Tailings	0.30	0.44	95.20	0.0338	5.34×10^{-10}	1.59×10^{-8}	0
Sand	0.45	0.30	24.60	0.2284	1.54×10^{-6}	6.75×10^{-6}	0
Case C							
Sand	0.30	0.33	5.00	0.3140‡	3.56×10^{-6}	1.13×10^{-5}	0
Tailings	0.80	0.44	85.00	0.0770‡	1.61×10^{-8}	2.09×10^{-7}	†
Sand	0.50	0.40	15.00	0.3418‡	3.12×10^{-6}	9.14×10^{-6}	0

† Three different values: 3.17×10^{-8}, 1.59×10^{-7}, and 4.76×10^{-7} s^{-1}.

‡ Slightly different from that used in this example.

This example focuses on the scenarios found in Case C, which include consumption of oxygen within the tailings layer. The one-dimensional domain consists of a top-to-bottom sequence of sand, tailings, and sand with thicknesses of 0.30, 0.80, and 0.50 m, respectively. The volumetric water content of each layer is set constant using layer-specific pore-water pressure boundary conditions. The file also includes a more realistic approach to generating the pore-water pressure profile for those wanting to model more advanced scenarios that consider such processes as transient changes in the flow system and spatial variability in water contents under various infiltration scenarios. The volumetric water content functions are estimated using the sample sand and silt functions while the hydraulic conductivity functions are estimated using the Fredlund-Xing-Huang model with a saturated hydraulic conductivity of 5×10^{-5}, 1×10^{-7} and 2×10^{-5} m/s for the upper sand, silt, and lower sand, respectively.

The bulk diffusion coefficient for oxygen transfer through the gas and dissolved phases are computed in a spreadsheet using Equation 8, the volumetric water content functions, and the reported values of the effective diffusion coefficient. Figure 1 shows the bulk diffusion coefficient through the gas phase versus the volumetric air content. Figure 2 shows the bulk diffusion coefficient through the dissolved phase versus the volumetric water content. The bulk reaction rate coefficients are computed using the effective reaction rate coefficients found in Table 1 and the equivalent diffusion porosity, which is calculated using Henry's dimensionless equilibrium constant. This latter constant is calculated as the ratio of concentration in the water phase to the concentration in the air phase, which is approximately equal to 0.032 at 20°C. This constant is used in all calculations and leads to slight differences between calculated and reported values of equivalent diffusion porosity.

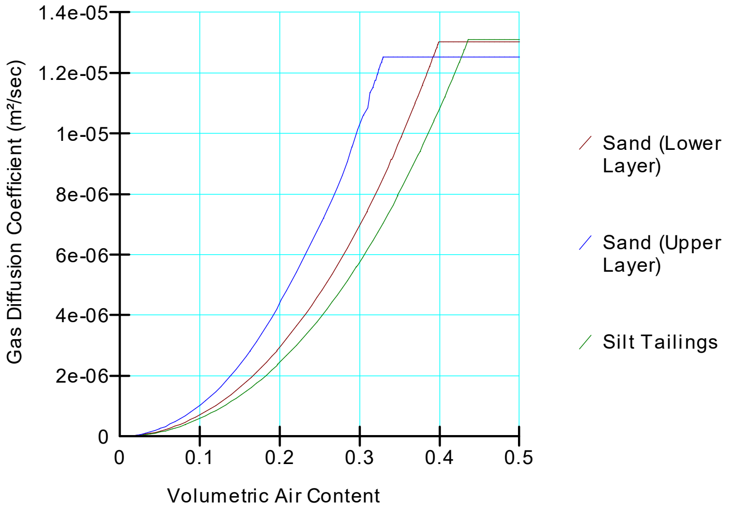

Figure 1. Bulk diffusion coefficient through the gas phase.

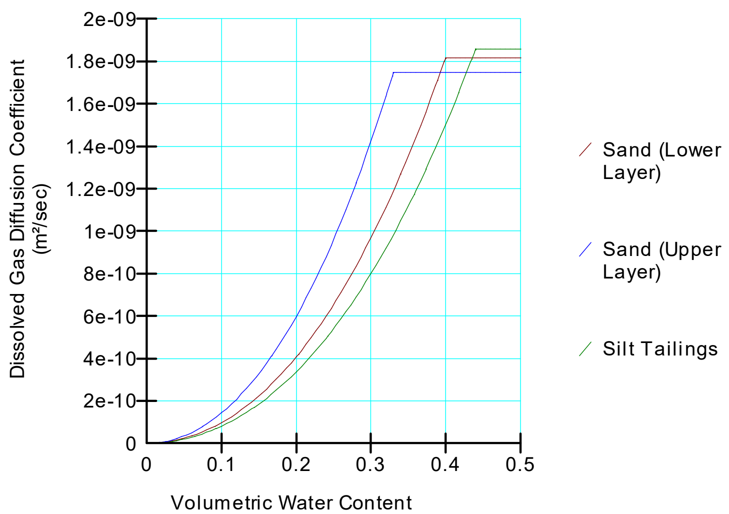

Figure 2. Bulk diffusion coefficient through the dissolved phase.

The oxygen concentration at the upper boundary is set equal to 276 g/m³. Oxygen consumption in the mine waste beneath the base of the cover is assumed to maintain the oxygen concentration at 0.0 g/m³. Although this is not strictly correct, Mbonimpa et al. (2003) note that this condition is the worst-case scenario for evaluating the effectiveness of the oxygen barrier. Initial conditions for the transient gas transfer analyses are established using an activation concentration of 0.0 g/m³.

Oxygen transport and/or consumption are modeled for 40 days using 960 timesteps. The analysis involving the non-reactive tailings are solved using a linear timestep sequence while the analyses with reactive tailings are solved using an exponential timestep sequence. An exponential timestep sequence was not used for the analyses involving consumption for reasons that are discussed subsequently.

Results and Discussion

Figure 3 shows the volumetric water content, volumetric air content, and equivalent diffusion porosity profiles. The porosity of the silt is equal to 0.44 while the simulated volumetric water content is equal to 0.374, making the volumetric air content equal to 0.066. The resulting equivalent diffusion porosity (computed with Equation 2) is 0.078, which compares very well to that found in Table 1.

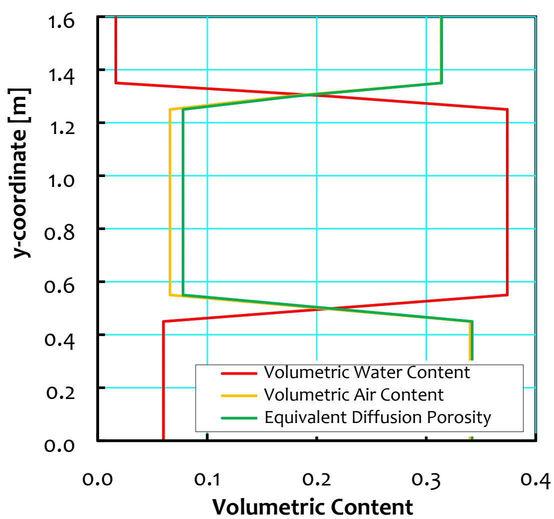

Figure 3. Volumetric content profiles.

Figure 4 shows the bulk and effective diffusion coefficient profiles. The effective diffusion coefficient through the silt material is equal to 1.61×10^{-8} m²/s, which is equal to that found in Table 1. This effective diffusion coefficient is approximately two orders of magnitude greater than that in the overlying and underlying sands. The magnitude of the bulk diffusion coefficient through the dissolved phase is approximately two orders of magnitude smaller than that through the gas phase, which does little to diminish the effectiveness of the oxygen barrier.

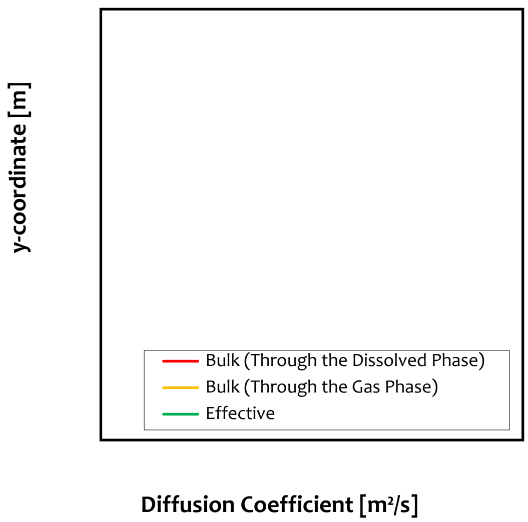

Figure 4. Bulk and effective diffusion coefficient profiles.

Figure 5 shows the steady-state concentration profiles in the presence of non-reactive and highly reactive tailings. The top-down consumption of oxygen in the highly reactive tailings produces an ever-decreasing concentration, which results in a bow in the steady-state concentration profile. This is similar to that observed in systems in which advection transport is in the opposite direction of the diffusion transport.

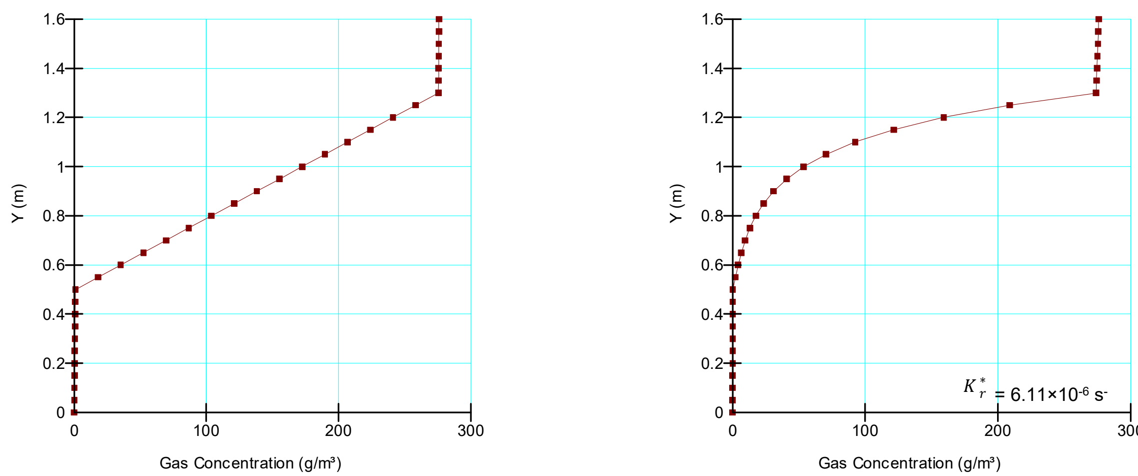

Figure 5. Steady-state concentration profiles for non-reactive (left) and highly reactive tailings (right).

Figure 6 shows the simulated oxygen fluxes at the base of the cover for the various scenarios. As expected, the results are in very close agreement with those of the analytical solution (Mbonimpa et al., 2003). Oxygen consumption in the tailings clearly reduces the oxygen flux past the base of the cover. Figure 7 shows the oxygen flux into the top and out of the bottom of the reactive tailings layer. Naturally the flux into the top of the cover increases as the tailings become more consumptive despite the decrease in the flux out of the bottom.

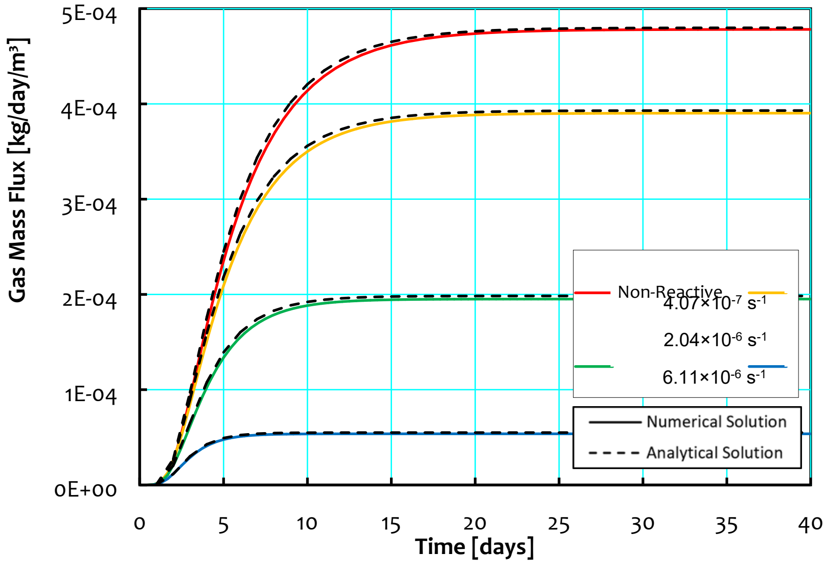

Figure 6. Oxygen flux at the base of the cover for various values of the bulk reaction rate coefficient.

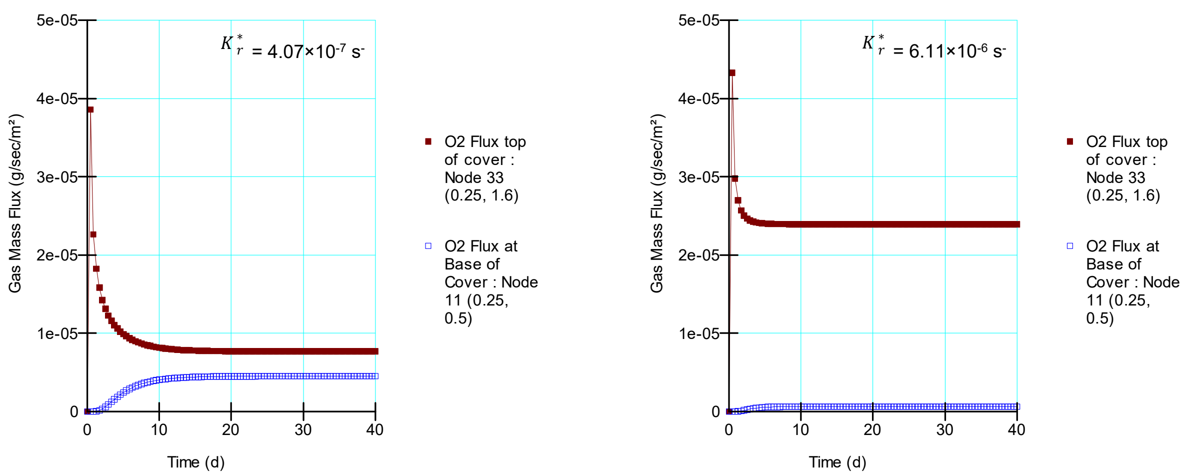

Figure 7. Oxygen flux entering and leaving the slightly reactive (left) and highly reactive tailings (right).

As previously noted, exponential time sequences were not used for the analyses involving consumption. Subtle inaccuracies developed in the solution because the oxygen consumption rates (last term in Equation 5) were being multiplied by increasingly larger time increments. Consumption across the step had to be met by diffusion influx of oxygen, which produced subtle variations in the concentration profiles from time step to time step. The inaccuracies only became noticeable for the case involving the largest amount of oxygen consumption. Regardless, a linear time stepping sequence was used in all cases.

Summary and Conclusion

SEEP/W and CTRAN/W can be used to study the effectiveness of cover systems with capillary barrier effects at limiting oxygen ingress into sulphide bearing mine wastes. Cover systems of this nature rely on the presence of a layer that remains close to full saturation. Consideration can also be given to the effectiveness of adding different quantities of reactive materials to the cover system. Often the greater challenge in designing these cover systems is ensuring saturation in the water retention layer when the cover is subjected to highly variable climate conditions. A SEEP/W analysis that makes use of a land-climate interaction boundary condition could be used to explore changing moisture conditions within the cover due to variable climate conditions.

References

Aachib, M., Mbonimpa, M., and Aubertin, M. 2004. Measurement and prediction of the oxygen diffusion coefficient in unsaturated media, with applications to soil covers. Water, Air, and Soil Pollution, 156(1): 163-193.

Mbonimpa, M., Aubertin, M., Aachib, M., and Bussière, B. 2003. Diffusion and consumption of oxygen in unsaturated cover materials. Canadian Geotechnical Journal, 40(5): 916-932.